# PART V

## Coastal Processes and Sediment Transport

*"T" Groins and Nourishment Protecting Coastal Railway*

# CHAPTER 146

## OBSERVATIONS OF GRANULAR-FLUID MIXTURE UNDER AN OSCILLATORY SHEET FLOW

by

Toshiyuki Asano[1]

### 1. Introduction

Sediment transport due to wave action has been classified into three modes; bed load over a practically flat bed under small tractive force, suspended load over a rippled bed under moderate shear stress, and sheet flow under high shear stress where ripples are washed out. Studies of the sheet flow have recently received much attention because a large amount of sand is transported under this mode. However, sheet flow is a grain-fluid mixture flow of high concentration, thus the mechanism is more complex than that of the other two modes. In the sheet flow region where several layers of grains are mobilized, grain to grain collision performs a main role in the momentum exchange. The relationship between the applied stress and the bulk deformation is not a Newtonian, and depends on the grain concentration and the rate of deformation.

Hanes - Bowen(1985) have proposed a granular - fluid model to describe intense bed - load transport in an uni-directional flow. In their model, the flow is divided into two regions; grain collision dominated granular fluid region, and fluid stress dominated fluid shear region. They have derived a relation mathematically between the grain transport rate and applied shear stress.

Shibata - Mei(1986) have proposed another granular - fluid model in so-called macro viscous region where the shear rate is low and granular friction is as important as granular collision. Mathematical expressions to describe velocity profiles and granular discharge have been deduced.

These studies provide physical insight into the mechanism of sheet flow, however, the results are not able to be applied directly because the oscillatory sheet flow is a dynamic process under an unsteady flow.

[1]Dept. of Ocean Civil Engineering, Kagoshima University, Korimoto 1-21-40, Kagoshima, 890, Japan

The author (1990) has proposed a two-phase model for oscillatory sheet flow based on the conservation of mass and momentum for fluid and sediment. The model provides the quantitative description on the sheet flow properties, however, reliable experimental data are essentially required to examine the validity of the model. Since the mechanism of time varying grain densely mixed flow is highly complicated, clear experimental understandings have not sufficiently been obtained.

Even for macroscopic properties, there is much difference among reported results. For example, Horikawa et al.(1982) reported that their data on sediment transport rate agree well with Madsen - Grant formula in which the sediment transport rate is proportional to the 3rd power of the Shields number. Meanwhile, Sawamoto-Yamashita(1986) reported to the 1.5 power relationship between the sediment transport rate and Shields number.

In the present paper, detailed measurements on the intrusion depth of the sheet flow, sediment transport velocity and concentration etc. are carried out in order to obtain basic data which are useful to investigate the flow mechanism of oscillatory sheet flow.

## 2. Experimental Apparatus

An oscillatory flume capable of generating oscillatory sheet flows was constructed. The flume illustrated in Fig.1 is 8.0m long for horizontal section and 2.5m high for vertical section. The total length of the water column when the flume is filled is 10.2m including the joint section. The natural frequency of the oscillation calculated by the total length is 4.53sec. The horizontal section was made of clear acrylic which allows direct visual observation, and has a 15cm × 15cm square cross-section. The bottom of the central section is depressed to form a bed material container which is 1.8m long and 5.0cm deep. The oscillatory flows were generated via a piston driven by an electric servo motor and a drive shaft.

For the convenience of video frame tracing analysis, large and light plastic particles, 4.17mm in diameter and 1.24 in specific gravity, were used. Some parts of the particles were painted in various colors, and the water in the flume was also dyed in order to obtain clear pictures. Motion of the particles under oscillatory flows was taken with a high speed video camera at an exposure speed of 1/1000 sec, and also taken with a 35mm motor-driven camera as an auxiliary.

During one experimental run, special attention is paid to maintain the upper surface of the particle assembly flat and uniform in the flow direction. Keeping it uniform over a long time was found to be difficult because a large amount of particles is moved under sheet flow condition. Consequently, an oscillatory flow was generated just for 2 periods for each run, the data from the second half to the fourth half period in which uniformity of the flow had been assured was used for the analysis.

Table 1 shows the experimental conditions. The Shields number, $\Psi$ in the table was tentatively calculated by assuming a friction factor f=0.01, since the movable bed friction under oscillatory flows is not sufficiently understood yet.

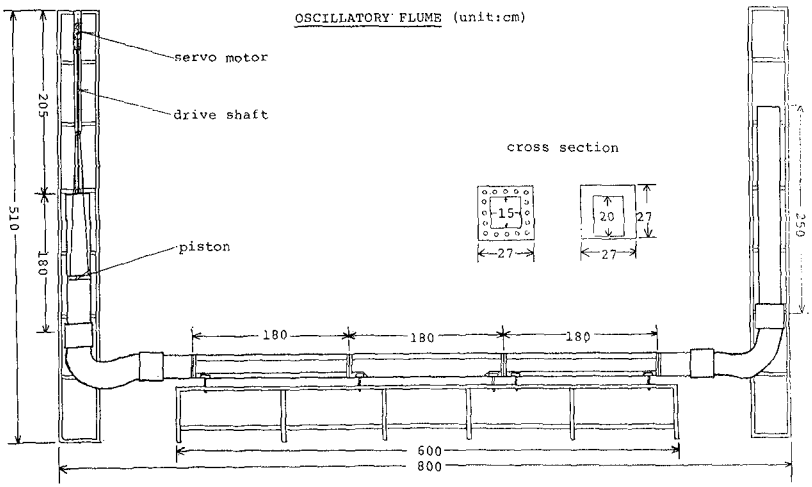


Figure 1: Oscillatory Flume

Table 1: Experimental Conditions

| | T (sec) | $\hat{U}$ (cm/s) | $\Psi$ |
|---|---|---|---|
| CASE-1 | 4.64 | 73.94 | 0.279 |
| CASE-2 | 4.64 | 96.85 | 0.478 |
| CASE-3 | 4.98 | 101.25 | 0.523 |
| CASE-4 | 5.28 | 83.04 | 0.352 |
| CASE-5 | 5.44 | 63.07 | 0.203 |
| CASE-6 | 4.35 | 76.35 | 0.297 |
| CASE-C1 | 4.64 | 92.60 | 0.437 |
| CASE-C2 | 4.64 | 85.04 | 0.369 |
| CASE-C3 | 5.01 | 54.43 | 0.151 |
| CASE-C4 | 4.28 | 63.72 | 0.207 |

### 3. Experimental results

(a) particle motion

Picture-1 shows the behavior of the particles every 0.5sec. The period of this run(Case-C1) is 4.64sec, so that these six pictures cover over a little more than half a period. The indicator attached beneath the bottom shows the water surface level in the right vertical flume section.

The indicator in Picture (a) shows that the water level in the right vertical section rises to the maximum. In this phase, the flow velocity becomes zero, and the pressure gradient is the maximum. The particles have already started to move due to the pressure gradient. In the phase (b), the thickness of the sheet flow grows larger and moving velocity also increases. The particles move in saltation mode in the flow region $z > 0$, and move in sheet flow mode in the region $z < 0$, where a datum level (z=0) is taken as an upper surface of the particle assembly under still water condition. Although the flow velocity increases toward phase (c) and takes the maximum between phases (c) and (d), the particle velocity starts to decrease in the sheet flow layer $z < 0$, meanwhile the particles maintain large velocity in the saltation layer $z > 0$.

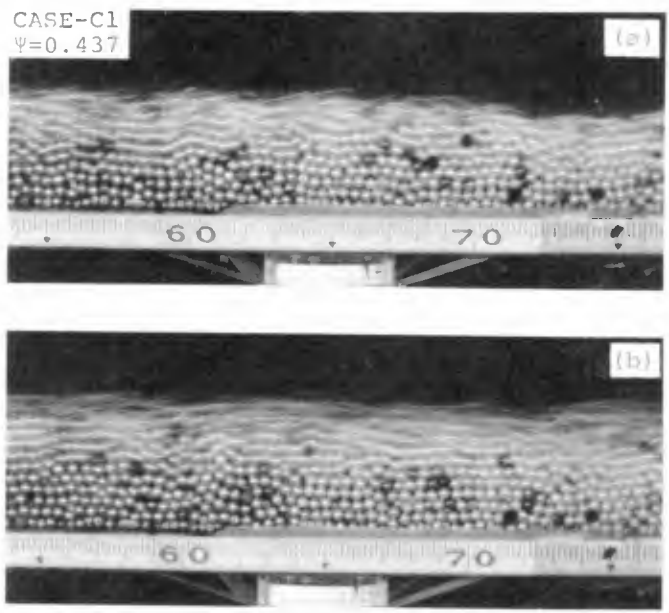


Picture-1 Sheet Flow and Saltation Motion under an Oscillatory Flow (CASE-C1)

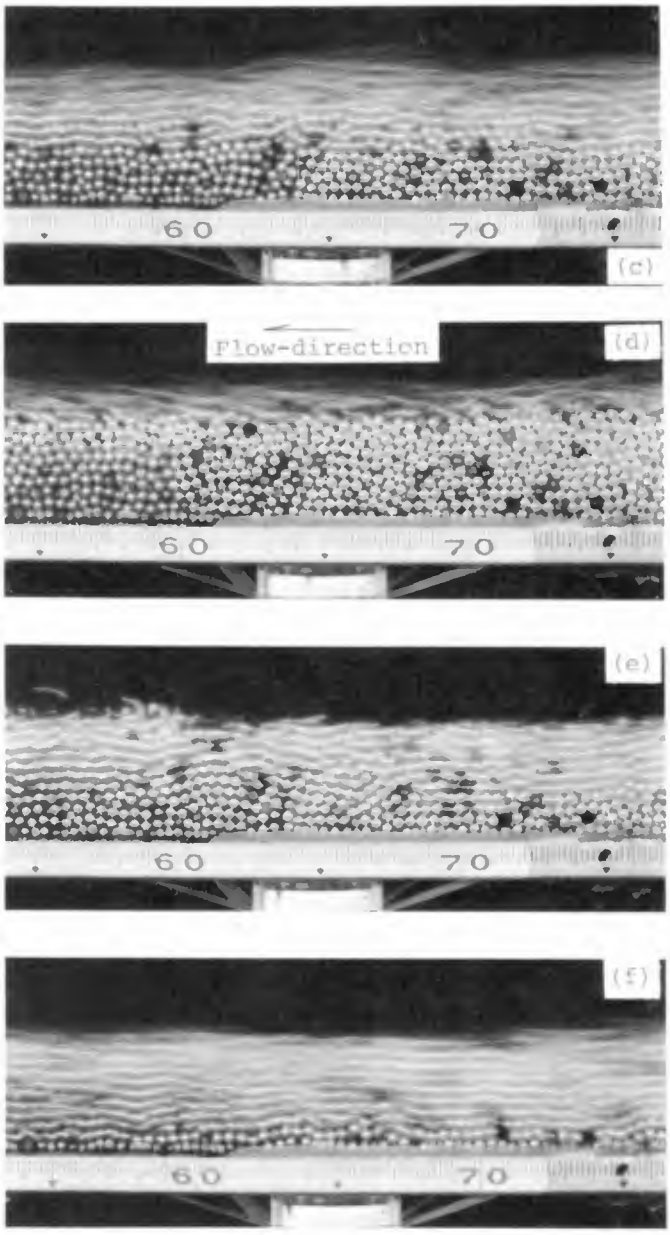


Picture-1 Sheet Flow and Saltation Motion under an Oscillatory Flow (CASE-C1) (Continued)

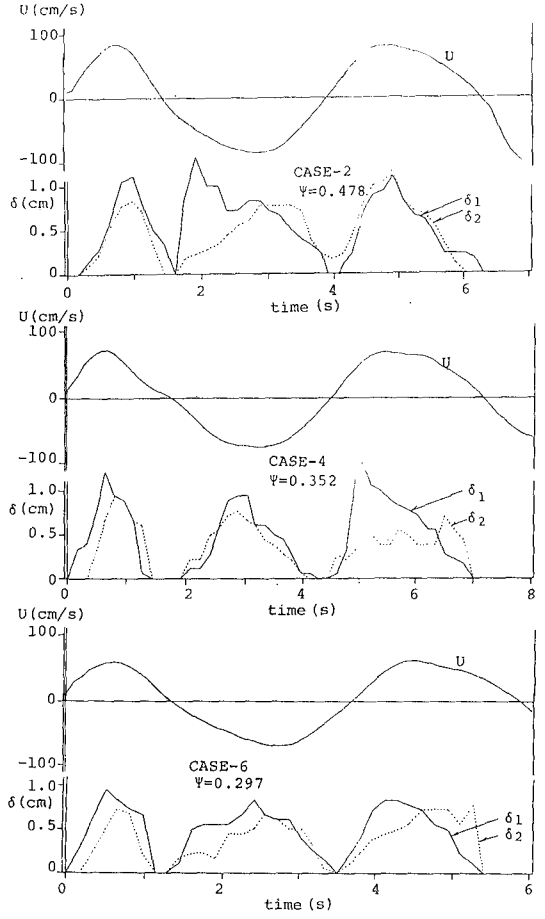


Figure 2: Temporal variations of thickness of sheet flow layer $\delta_1$ and saltation layer $\delta_2$

In the phase (e), particles in the sheet flow layer turn the direction to the right due to the pressure gradient although the mean stream velocity still moves from right to left. Some particles near z=0 are found to rotate because the flow direction may change there. In the phase (f), the thickness of the sheet flow layer starts to increase again.

In brief, the particle motion shows remarkable phase precedence from mean stream flow due to pressure gradient in the sheet flow layer, but relatively small phase precedence in the saltation layer.

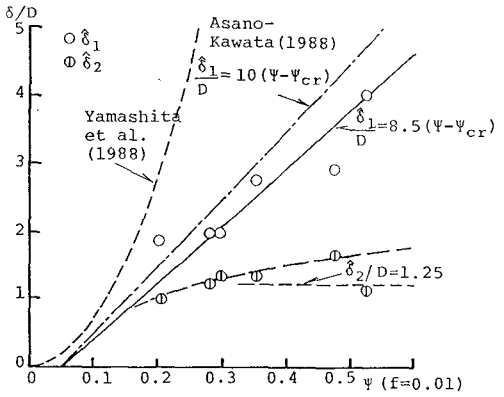


Figure 3: $\hat{\delta}_1$, $\hat{\delta}_2$ vs Shields number $\Psi$

(b) Thicknesses of Sheet flow layer and Saltation layer

A sheet flow layer thickness $\delta_1$ is determined by an intrusion depth of moving particles below the datum level(z=0), and the saltation layer thickness $\delta_2$ is defined by the maximum jumping height upward from z=0. Fig. 2 shows the phase variation of $\delta_1$ and $\delta_2$.

Fig. 3 shows the measured maximum thicknesses during half an oscillatory period $\hat{\delta}_1$, and $\hat{\delta}_2$ in relation to the Shields number $\Psi$ for CASE- $1 \sim 6$. The sheet flow layer thickness $\hat{\delta}_1$ increases almost linearly with the Shields number, and shows good agreement with the relation which the author proposed(1990). The relation that $\hat{\delta}_1$ is proportional to the applied shear stress has been confirmed by Hanes and Bowen(1985) and Wilson(1984), although their data were obtained in uni-directional flows.

Meanwhile, the maximum saltation layer thickness $\hat{\delta}_2$ increases gradually with the Shields number. The rate of increase is, however, small compared to results of stationary saltation for uni-directional flows( for example; Tsuchiya 1969). The reason why the difference arises is explained as follows: The momentum of a successively saltating particle increases with the number of times of saltation, however, the number is restricted under an oscillatory flow because the change of flow direction forces a saltating particle stop every half a period. Moreover, under sheet flow condition, the bed itself, on which a saltating particle collides and rebounds, moves as a sheet flow layer, so that a colliding particle does not receive enough momentum at the collision.

The thickness of the sheet flow layer might be governed by the dynamic Coulomb yield criterion which states the proportion between a shear stress

and a normal stress acting on a plane. The normal stress which consists of static pressure of the particle lattice, dispersive pressure due to particle collision and pore-fluid turbulence stress, balances not instantaneously but time-averagingly with the immersed weight of grains above. Applying the criterion at the boundary between mobile and immobile layers yields the following relation.

$$\tau_{-\delta_1} = \int_{-\delta_1}^{0} \rho g(s-1)c \, dz \, \tan\phi_r \tag{1}$$

in which, $\phi_r$ is the critical dynamic angle of internal friction. For the simplicity, the profile of sediment concentration $c$ is herein assumed to be uniform throughout a sheet flow layer. After some algebra of Eq.(1), the thickness of the sheet flow layer is given as a function of the Shields number $\Psi = u_*^2/\{g(s-1)D\}$ as follows.

$$\frac{\delta_1}{D} = \frac{\Psi}{\bar{c}\tan\phi_r} \tag{2}$$

In an oscillatory sheet flow, the angle of internal friction may be varied between an initial yield angle and an dynamic yield angle reflecting the flow unsteadiness. Tentatively adopting $\phi_r = 26.5°$ constant over a period, and $\bar{c} = 0.40$ provides,

$$\frac{\delta_1}{D} = 5.0\Psi \tag{3}$$

This coefficent 5.0 is found to be the same order as the value 8.5 obtained in the experiment in Fig. 3.

(c) Sediment Transport Velocity

The profiles of the horizontal particle velocity when the velocity becomes the maximum are shown into a non-dimensional form in Fig. 4. The figure shows that the velocity profile is upward convex, and approximately expressed by 1.5 power of $z/\delta_1$.

To visualize the velocity profile, additional experiments are performed in which white and red painted granulars are placed separately before generating an oscillatory flow. Picture-2 shows the results. The boundary is found to be upward convex, which coincides with the property of velocity profile illustrated in Fig. 4.

Fig. 5 shows the phase variations of the sediment transport velocity and mean stream velocity.

(d) Particle concentration

Instantaneous particle concentration was measured by counting the particles adjacent to the side wall within vertically divided grids. Fig. 6 shows the profiles of particle concentrations at the phase when mean stream velocity

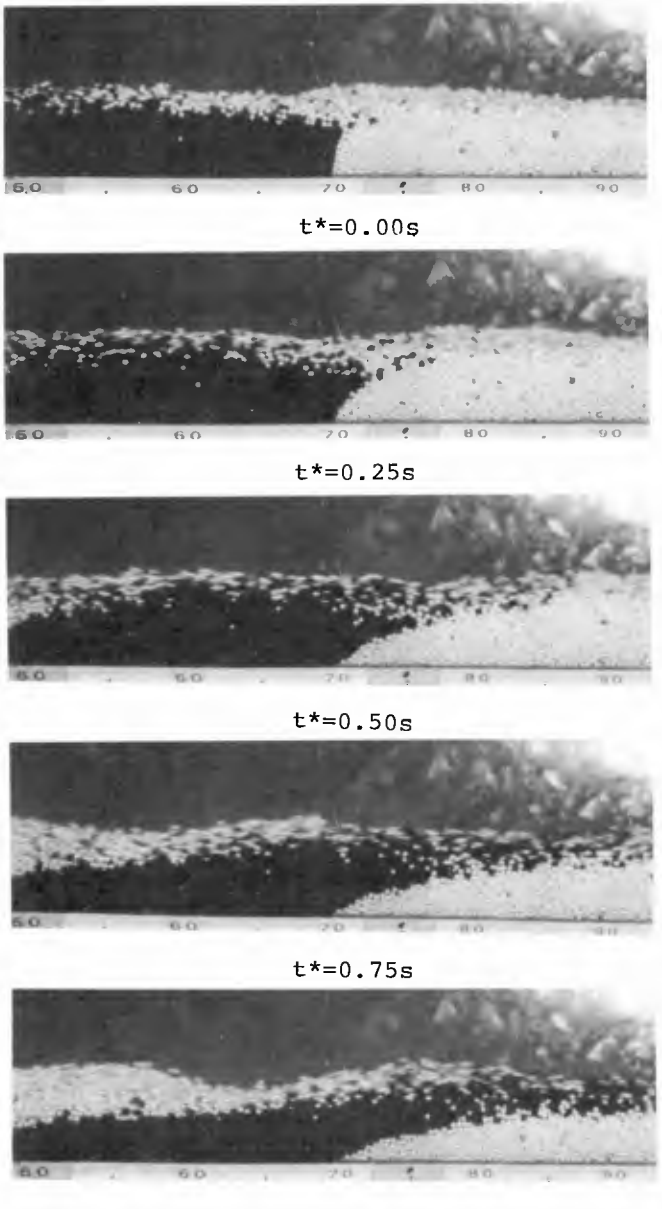


Picture-2 Particle Movements in a Sheet Flow Layer
(CASE-B5, T=4.60sec, $\hat{U}$ = 91.3cm/sec, $\Psi$ =0.425)

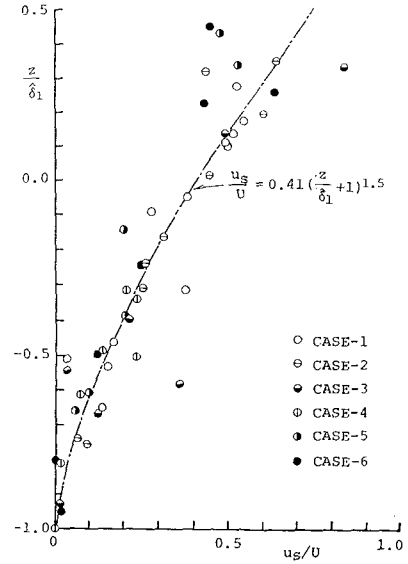


Figure 4: Profiles of Sediment Transport Velocity

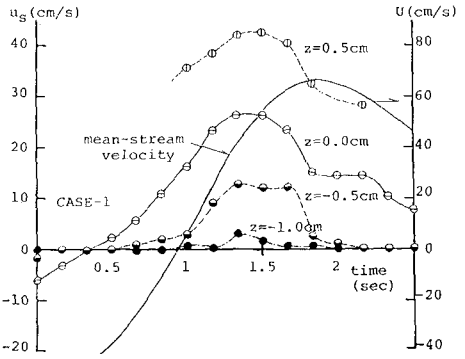


Figure 5: Phase Variations of Sediment Transport Velocity

becomes the maximum. The profiles are approximately expressed by upward convex curves in the sheet flow layer and by exponentially decay curves in the saltation layer. The curves in Fig. 6 show calculated concentrations using Eqs.(9) and (10) described later.

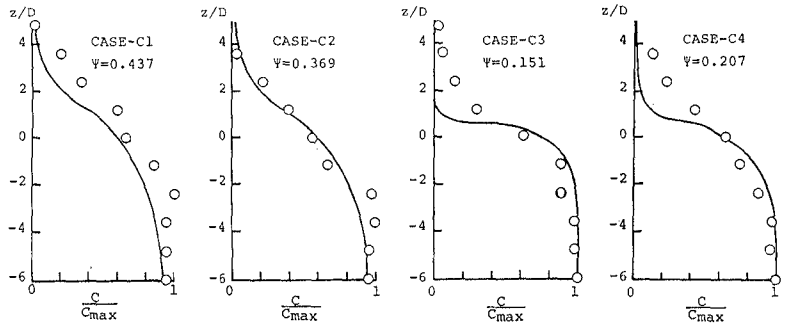


Figure 6: Profiles of Sediment Concentration at phase $\pi/2$

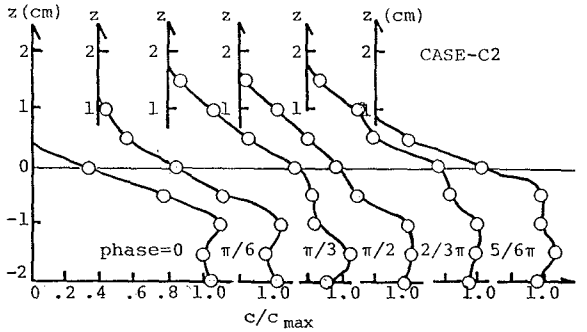


Figure 7: Phase Variation of Sediment Concentration Profile

The phase variations of the profiles are illustrated in Fig. 7.

Fig. 8 shows that the phase variation of the concentration at the boundary between the sheet flow layer and saltation layer; z=0.5cm. The reason why z=0.5cm is adopted here as the boundary is that the dilatancy of the particle assembly raises the boundary by around one particle diameter. This large dilatancy results from relatively large spheres used in the experiments as the bed material. If ordinary sea bed sand is used, the dilatancy effect would not arise so noticeably. Estimated concentration according to Engelund-Fredsøe(1976) formula is also drawn in the figure, which is originally proposed for an uni-directional flow.

## 4. Sediment Transport Rate

In this section, the relation between sediment transport rate $Q$ and the Shields parameter $\Psi$ is considered by synthesizing the above results.

The non-dimensional sediment transport rate during a half cycle is calculated as follows.

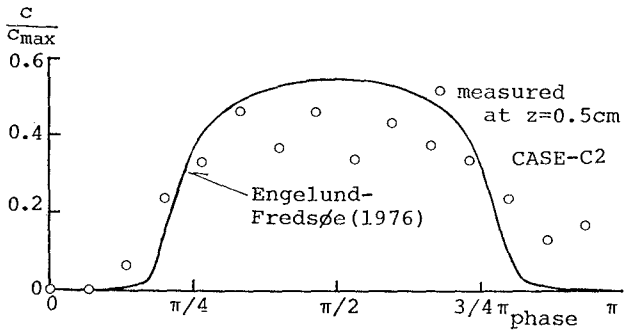


Figure 8: Phase Variation of Sediment Concentration at z=0.5cm

$$Q = \frac{q}{w_0 D} = \frac{\hat{U}}{\pi w_0} \int_0^{\pi} \int_{-\delta_1(t)/D}^{\hat{\delta}_2/D} c(z,\theta) \frac{u_s(z,\theta)}{U} dz^* d\theta \tag{4}$$

where, $w_0$ is the fall velocity of a particle, $z^*$ is $z/D$, $\hat{U}$ is the amplitude of mean stream fluid velocity expressed as a function of $\Psi$ as follows.

$$\hat{U} = \sqrt{2(s-1)gD\Psi/f} \tag{5}$$

First, based on the results in Fig. 3, the thicknesses of the sheet flow layer $\delta_1(t)$ and saltation layer $\hat{\delta}_2$ are assumed to be given by,

$$\delta_1(t)/D = 8.5[\Psi(t) - \Psi_{cr}] = 8.5[\Psi \sin^2 \sigma t - \Psi_{cr}] \tag{6}$$

$$\hat{\delta}_2/D = 1.25 \tag{7}$$

According to the results in Fig. 4, the sediment transport velocity $u_s$ is given by,

$$\frac{u_s(t)}{U} = 0.41\left(\frac{z}{\delta_1(t)} + 1\right)^{1.5} \sin \sigma t \tag{8}$$

Concerning the particle concentration, the following profiles are assumed.

$$c = c_{max} - \{c_{max} - c_B(t)\} \exp(\alpha_1 z^*) \qquad z^* < 0 \tag{9}$$

$$c = c_B(t) \exp\{-\alpha_2 z^*\} \qquad z^* > 0 \tag{10}$$

in which, $z^* = z/D$, $\alpha_1 = D/\delta_1(t)$, $\alpha_2 = D/\hat{\delta}_2$, and $c_{max}$ is the maximum concentration (here, 0.65 is used). The time dependent concentration $c_B(t)$ at the datum level is given by Engelund - Fredsøe formula. The calculation of Eq.(4) is carried out using the present experimental condition; s=1.24, D=4.17mm. The friction factor is given by constant 0.01.

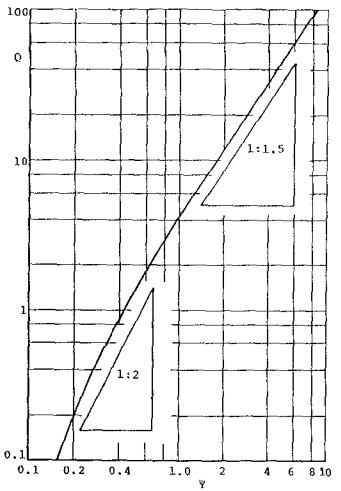


Figure 9: Calculated Non-dimensional Sediment Transport Rate

The calculated sediment transport rate $Q$ shown in Fig. 9 is found to be proportional to the 3/2 power of the Shield number if $\Psi$ is greater than around 0.8, and the power approaches to 2 with decrease of $\Psi$. This result is explained as follows. The sheet flow layer thickness $\delta_1(t)$ which occupies most of the integral range is found to be proportional to $\Psi$, and $u_s/U$ does not show clear dependence on $\Psi$, so that $u_s \sim U \sim \Psi^{1/2}$. Consequently, the sediment transport rate $Q$ is approximately proportional to the Shields number $\Psi$ raised to the 3/2 power. According to Engelund-Fredsøe formula $C_B$ also varies with $\Psi$, however, the dependence on $\Psi$ is little if $\Psi$ is greater than around 0.8.

## 5. Conclusions

(1) The particle motion is characterized by two modes; saltation mode above the datum level and sheet flow mode below that. The phase precedence of the particle motion against mean stream motion is becoming noticeable with entering downward in the sheet flow layer.

(2) The maximum thickness of the sheet flow layer is found to increase linearly with the Shields number, which is assured by simple kinematic model. Meanwhile, the maximum thickness of the saltation layer increases gradually with the Shields number.

(3) The profiles of the horizontal particle velocity at the phase of the maximum mean flow velocity are expressed by upward convex curves expressed

by 1.5 power of $z/\hat{\delta}_1$.

(4) The particle concentration is approximately described by a simple profile proposed here, where the concentration at datum level is given by Engelund-Fredsøe formula.

(5) Summarizing the above results, a semi-empirical relation between sediment transport rate $Q$ and the Shield number $\Psi$ is proposed. The sediment transport rate is found to be proportional to $\Psi$ raised to the 1.5 power for large tractive force $\Psi > 0.8$.

## AKNOWLEDGEMENT

The author wishes to express his appreciation to Mr. Kazuo Nakamura, technician of Dept. of Ocean Civil Engrg., Kagoshima Univ. for designing and fabricating the electronic driving unit of oscillatory flow. The author also expresses his thanks to Mr. Yasuhiro Nakano and Mr. Toshimitsu Takazawa, former students; and to Mr. Kenji Tamai, graduate student of Ocean Civil Engrg., Kagoshima Univ. for their help in performing experiments and data analyses.

This research is partly sponsored by the Grant-in Aid for Scientific Research of the Japanese Ministry of Science, Culture and Education.

## REFERENCES

Asano T. (1990): Two-phase flow model on oscillatory sheet flow , Proc. of 22nd ICCE, pp.2372-2384.

Engelund F. and J. Fredsøe (1976): A sediment transport model for straight alluvial channels, Nordic Hydrology, Vol.7, pp.293-306.

Hanes D. M. and A. J. Bowen (1985): A granular-fluid model for steady intense bed-load transport, J. of Geo. Res., Vol.90, No. C5, pp.9149-9158.

Horikawa K, A. Watanabe and S. Katori (1982): Sediment transport under sheet flow condition, Proc. 18th ICCE, pp.1335-1352.

Sawamoto M. and T. Yamashita (1986): Sediment transport rate due to wave action, J. of Hydroscience and Hydraulic Engineering, Vol.4, No.1, pp.1-15.

Shibata M. and C. C. Mei(1986): Slow parallel flows of a water - granule mixture under gravity, Part I and II, Acta Mechanica, Vol. 63, pp.179-216.

Tsuchiya Y. (1970): On the mechanics of saltation of a spherical sand particle in a turbulent stream, Proc. 13th Cong. IAHR, Vol.2, pp.191-198.

Wilson K.C. (1984): Analysis of contact load distribution and application to deposit limit in horizontal pipes, J. of Pipelines, Vol.4, pp.171-176.